

# Temperature Profile Retrieval from Surface to Mesopause by combining GNSS Radio Occultation and passive microwave Limb Sounder Data

Axel von Engel<sup>1,2</sup>, Stefan Bühler<sup>1</sup>, Gottfried Kirchengast<sup>2</sup>, and Klaus Künzi<sup>1</sup>

**Abstract.** A theoretical study on the combination of a passive microwave and a GNSS radio occultation instrument, mounted on the International Space Station (ISS), was performed. Both instruments allow to deduce the atmospheric temperature profile. We combined realistically simulated data of the two highly synergistic sensors with the optimal estimation method (OEM) and retrieved single joint temperature profiles from 0 to 90 km altitude for which we found accuracies  $< 1$  K below 35 km and  $< 4$  K in the mesosphere, respectively. In addition, we performed simultaneous tropospheric water vapor and temperature retrievals leading to a water vapor accuracy  $< 10$  to 20% at altitudes below 5 to 8 km. The OEM allows to optimally exploit the synergy in the data and maximizes retrieval accuracy over the full range from surface to mesopause. It seems worthwhile to install this type of instrument combination on the ISS or other low-Earth-orbit (LEO) platforms.

## Introduction

Using a radio occultation instrument (ROI) for tracking GNSS (U.S. Global Positioning System, GPS, or Russian Global Navigation Satellite System, GLONASS) satellite signals in limb geometry is a relatively new method to probe the terrestrial atmosphere by exploiting the change in refractivity with altitude. The technique has been demonstrated with the GPS Meteorology (GPS/MET) instrument [Ware *et al.*, 1996; Kursinski *et al.*, 1997]. The main source of geophysical information is the varying density in the atmosphere. Contributions from water vapor (WV) must be taken into account at tropospheric altitudes. One can derive temperature information at altitudes of about 0–50 km, and WV at altitudes below 5–8 km.

Probing the atmosphere with a passive microwave instrument (PMI) in limb geometry is a well developed technique. In general one observes the emissions of rotational transition lines of the species of interest. The observed intensity depends on the temperature and the volume mixing ratio (VMR) of the species observed. Temperature information

can be gathered particularly easily from oxygen lines, because the VMR profile is well known. Oxygen has a number of spin flip transitions around 60 GHz, the strongest ones allow temperature profile retrieval up to altitudes of 90 km, as shown with the Millimeter-Wave Atmospheric Sounder (MAS) [von Engel *et al.*, 1998]. The observation of strong oxygen lines in this 60 GHz cluster is usually limited to altitudes above the tropopause, because the limb path becomes opaque at lower altitudes.

The derivation of the temperature profile from microwave radiances is generally performed with an *a priori* constraint. A well suited method for the combination of a measurement and an *a priori* constraint is the OEM, which offers in addition a rigorous error analysis methodology [Rodgers, 1990]. ROI data allow a direct inversion.

The combination of PMI and ROI data permits the determination of a continuous temperature profile covering the altitude range from 0 to 90 km and was studied in connection with a possible MAS Follow-on mission on the ISS [Hartmann *et al.*, 1997].

## Instruments

Probing the Earth's atmosphere with a ROI is reviewed in Kursinski *et al.* [1997], focusing on the GPS/MET instrument. A raw level quantity measured is the atmospheric bending angle  $\alpha$ , which allows the derivation of the temperature and WV profile. Errors of  $\alpha$  vary with altitude, since different sources of error dominate at different altitudes [Kursinski *et al.*, 1997]. We assumed reasonable error characteristics which are in-between the "proof-of-concept" GPS/MET instrument and expected accuracies of modern receivers [GRAS-SAG, 1998]. Table 1 summarizes the  $\alpha$  error and the sampling (reflecting the resolution) of the measurement. Measurement errors were assumed to be unbiased (i.e., systematic errors are negligible), since this observation technique is self-calibrating. Useful determination of  $\alpha$  above 60 km is not possible, due to the poor signal-to-noise (S/N) ratio of mesospheric ROI data.

**Table 1.** Sampling grid used for the simulated measurements of the ROI, along with the corresponding bending angle errors assumed.

Height [km]	Sampling $dz$ [km]	Error [ $\mu$ rad]
$00 \leq z \leq 25$	0.25	4.0
$25 \leq z \leq 40$	0.50	2.8
$40 \leq z \leq 60$	1.00	2.0

<sup>1</sup>Institute of Environmental Physics, Univ. of Bremen, Bremen, Germany

<sup>2</sup>Institute for Geophysics, Astrophysics, and Meteorology (IGAM), Univ. of Graz, Graz, Austria

The instrument characteristics for the PMI have been derived from the MAS as flown on the Space Shuttle [Croskey *et al.*, 1992], with reasonable modifications, reflecting current technical advances [Bühler, 1999]. Only the temperature detection band around 61.15 GHz is used. Three different values have been set for  $T_{\text{sys}}$ , the system noise temperature: 500 K (modern double sideband receiver), and two values above and below: 1000 K and 250 K. An integration time of 0.3 s (MAS: 0.08 s) for a 1 km sampling grid was assumed, leading to moderately degraded horizontal resolution in comparison to the MAS, but resulting in an improved S/N ratio in the mesosphere. As a further improvement, a modern antenna has been assumed. The original MAS instrument allowed temperature retrieval with 10 km resolution in the mesosphere [von Engel *et al.*, 1998], with the improvements a resolution of 5 km is possible. Systematic PMI errors, expected to be small after proper pre-processing, have been disregarded in this study.

### Forward Model

The principle equations of the ROI forward model are given in e.g., Kursinski *et al.* [1997]; the calculation of the bending angle  $\alpha$  as a function of refractivity follows an Abelian integral equation, refractivity itself depends on pressure, temperature, and WV.

The forward model used for the PMI is a line-by-line radiative transfer model, which includes a model to calculate the magnetic field strength of the Earth, and the corresponding Zeeman splitting of the Oxygen lines. The radiative transfer for the Oxygen line at 61.15 GHz is performed polarized, all other lines are calculated unpolarized. For a more detailed description see von Engel *et al.* [1998].

### Inversion Model

The employed retrieval algorithm is based on the OEM, as reviewed by Rodgers [1990]. The inversion is non-linear and an iterative approach to minimize the difference between the simulated quasi realistic measurements and the forward modeled measurements is used. The minimum is found by calculating the derivative of the forward model with respect to the retrieval parameters, called the weighting function matrix  $\mathbf{K}$ . The matrix  $\mathbf{K}$  is calculated by perturbation.

In “dry” scenarios (WV ignored), the profile retrieved by the inversion algorithm is the temperature profile. In “wet” scenarios temperature and WV VMR profiles, along with a reference pressure at a certain altitude, are retrieved. The reference pressure is used to generate the pressure profile, using the hydrostatic equation. It is necessary in “wet” scenarios due to the high variability of tropospheric WV, affecting the pressure. It could also be introduced in “dry” scenarios to correct for attitude uncertainties of the sensor on the ISS; this would affect the temperature retrieval accuracy only marginally. The measurement vector consists of the data of the two instruments. The calculation of the  $\mathbf{K}$  matrix is performed with the two mentioned forward models, it completely separates into a ROI and a PMI part, respectively.

In both scenarios (“dry” and “wet”), the temperature profile is retrieved on a vertical grid with different stepwidths:

0.5 km: 0–30 km; 1 km: 30–40 km; 2.5 km: 40–60 km; 5 km: 60–90 km. This sampling has been determined by an optimization process, assuring that it reasonably matches the resolution available from the measurements. The highest sampling of 0.5 km reflects the expected vertical resolution of a ROI below 30 km. A vertical sampling of 1 km is suitable between 30 and 40 km, where the contribution from the ROI gradually decreases, but the PMI provides sufficient information. The major part of the information is coming from the PMI above 40 km, where a decrease of vertical sampling to 2.5 km is reasonable. Above 60 km all information comes from the PMI.

“Wet” scenarios were calculated for three cases (mid-latitude winter, mid-latitude summer, tropical). The WV VMR profile is retrieved between 0 and 8 km, with a vertical sampling of 0.5 km. Above, the contributions of WV to the bending angles  $\alpha$  are too small to allow meaningful retrievals. The reference pressure is retrieved at a mid-stratospheric altitude of 30 km.

The *a priori* error of the temperature profile varies with altitude, reflecting our typical prior knowledge of a temperature profile. We roughly follow the uncertainties published by Palmer *et al.* [2000]: the *a priori* uncertainty is set to 2 K for altitudes up to 16 km, above, it increases linearly with altitude to 20 K at 90 km.

The *a priori* error for the WV VMR profile was set to 30% relative uncertainty, the *a priori* error of the pressure value at 30 km to 10%.

### Simulation Setup

Both instruments were assumed to be mounted on the International Space Station (near-circular orbit at  $\approx 400$  km height with  $\approx 53^\circ$  inclination), reflecting a relevant ROI-PMI hybrid sensor proposal by Hartmann *et al.* [1997]. We assumed that both instruments are observing in opposite-flight direction, with the PMI continuously measuring the atmospheric emissions while the ROI acquires setting occultation events with a confined field of view of  $\pm 15^\circ$  in roughly the same atmospheric space. Perfect collocation is assumed in this study, while actual collocation is only given within  $\approx 500$  km at the tangent point. Mitigation of potential mis-location errors in the latter case is possible by incorporating *a priori* information on horizontal gradients (e.g., from atmospheric analyses or forecast fields).

The position and time of the occultation events as well as the quasi realistic bending angle measurements were computed with the End-to-End GNSS Occultation Performance Simulator, a ROI mission simulation software [Kirchengast, 1998]. More than 160 useful setting events of either GPS or GLONASS covering the required altitude range of 0 to 60 km were found for a single day. The PMI measurements were generated at the occultation locations.

For the investigation in this paper, 30 events out of the about 160 were quasi-randomly chosen, which cover the whole Earth appropriately and allow some statistics to be performed about the expected accuracy of the retrieval. The accuracy of the combined retrieval varies with location, owing to the varying temperature profile, the different magnetic field strengths, and the different observation geometries with

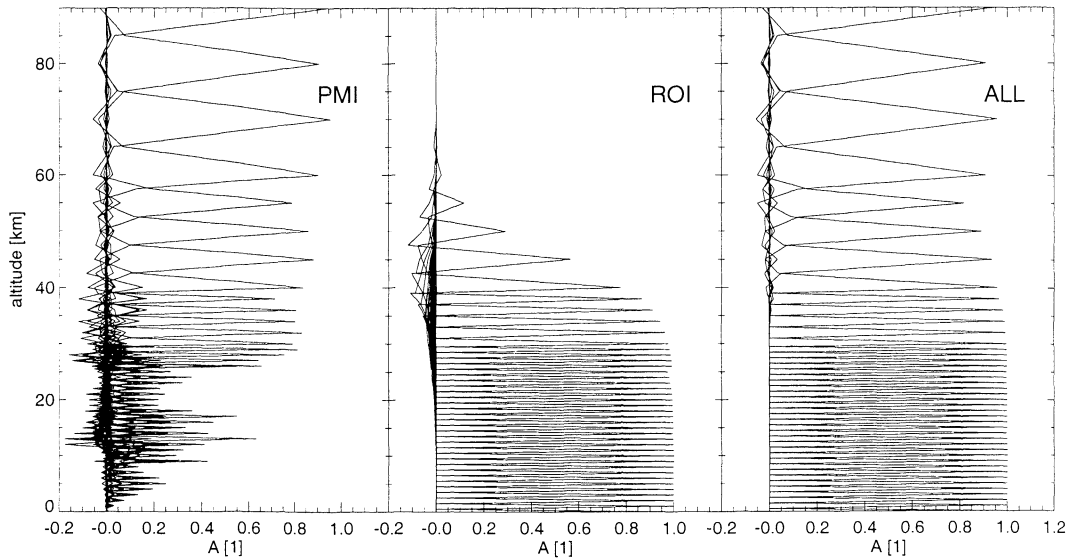


**Figure 1.** Rows (every 2<sup>nd</sup> row) of the “dry” temperature AKM for the passive microwave instrument (PMI), the radio occultation instrument (ROI), and both combined (ALL),  $T_{\text{sys}} = 500$  K.

respect to the magnetic field. In addition, in the “wet” scenario the temperature accuracy is affected by WV.

## Results

The averaging kernel matrix (AKM)  $\mathbf{A}$  gives information about the contributions of the *a priori* knowledge and the knowledge derived from the measurements of the combined ROI-PMI instrument [Rodgers, 1990].

The AKMs  $\mathbf{A}^{\text{ROI}}$  and  $\mathbf{A}^{\text{PMI}}$  for each instrument alone can be derived from the matrix  $\mathbf{K}$ , the *a priori* covariance matrix  $\mathbf{S}_0$ , and the measurement error covariance matrix  $\mathbf{S}_y$ , respectively, by separating them into a ROI part and a PMI part. First, the respective contribution function matrices  $\mathbf{D}$  are calculated by inserting the corresponding ROI and PMI sub-matrices of  $\mathbf{K}$  and  $\mathbf{S}_y$  in the formula

$$\mathbf{D} = (\mathbf{S}_0^{-1} + \mathbf{K}^T \mathbf{S}_y^{-1} \mathbf{K})^{-1} \mathbf{K}^T \mathbf{S}_y^{-1},$$

where  $\mathbf{K}^T$  denotes the transpose of  $\mathbf{K}$ . The matrices  $\mathbf{A}^{\text{ROI}}$  and  $\mathbf{A}^{\text{PMI}}$  are then calculated by

$$\begin{aligned} \mathbf{A}^{\text{ROI}} &= \mathbf{D}^{\text{ROI}} \mathbf{K}^{\text{ROI}}, \\ \mathbf{A}^{\text{PMI}} &= \mathbf{D}^{\text{PMI}} \mathbf{K}^{\text{PMI}}. \end{aligned}$$

These two matrices give information about the contributions of the individual sensors. The resulting matrix rows are shown in Figure 1 for the “dry” temperature scenario, along with the total AKM. Only every second retrieval level is plotted. Note: the total AKM  $\mathbf{A}$  is *not* the sum of these two matrices, since the information of both instruments is combined in an optimal way in this case. Nevertheless, the individual matrices visualize well where the major information comes from in terms of the single sensors.

Figure 1 shows that the information for the temperature retrieval below 25 km is essentially from the ROI. It is thus possible to omit these retrieval levels in the calculation of the  $\mathbf{K}^{\text{PMI}}$  matrix, hence significantly reducing calculation time.

The ROI-PMI combination allows a temperature profile retrieval resolution of 2.5 km between 40 and 60 km. The ROI determines the possible resolution of the ROI-PMI combination below 40 km, since the attainable resolution of a PMI is much lower. Here, the contributions from the PMI lead to higher retrieval accuracy.

The mean error of the “dry” temperature retrieval of all 30 selected events for different  $T_{\text{sys}}$  is shown in Figure 2 (top), along with the individual errors of the PMI and ROI, show-

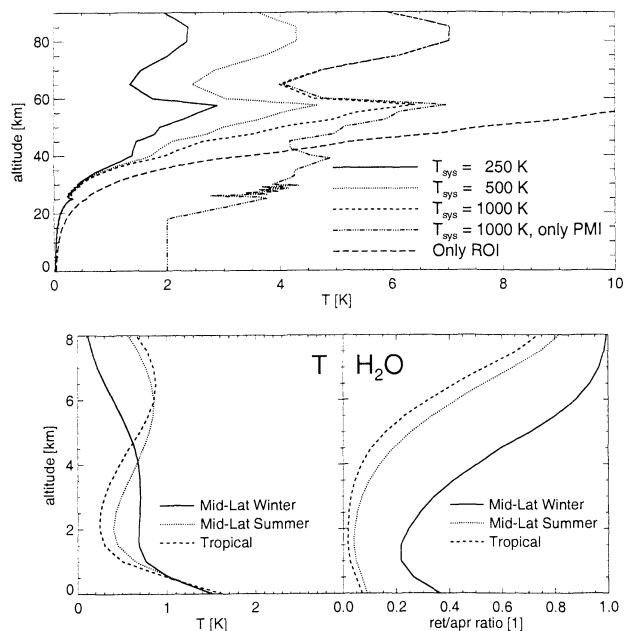


**Figure 2.** ROI and/or PMI temperature retrieval; Top: Mean error of the “dry” temperature retrieval of 30 events (Note: no PMI-only retrieval for  $\leq 25$  km, thus *a priori* values at these levels). Bottom: Errors of the “wet” scenarios, temperature retrieval errors (left), water vapor VMR retrieval error ratios (right) for three different atmospheres.

ing the improvement over individual retrievals; the mean error of the “wet” temperature retrieval and the error ratio for the WV retrieval are shown in the bottom panel. The error ratio is defined as the ratio of the retrieval error to the *a priori* error (the latter assumed 30 % as noted above).

A combination of a ROI and a PMI allows “dry” temperature retrieval up to 90 km, with a maximum error near 4 K, if a reasonably modern receiver with a  $T_{\text{sys}}$  value of 500 K is assumed. An improved receiver (for example cooled) with a  $T_{\text{sys}}$  value of 250 K improves the maximum error to near 2 K, since the S/N ratio is the major limiting factor for mesospheric temperature retrieval besides the narrowing lineshape with altitude. Mainly the ROI allows the derivation of the “dry” temperature profile for altitudes up to 35 km with an error below 1 K, as already found via validation of GPS/MET data [e.g., *Rocken et al.*, 1997].

The OEM allows a further separation of the error into a measurement and smoothing error, respectively. The former is caused by the measurement noise, the latter by smoothing as a result of the limited retrieval resolution [Rodgers, 1990]. In the  $T_{\text{sys}} = 1000$  K case the measurement error is the major error source up to altitudes of about 50 km (in the mesosphere the smoothing error is equally important), in the  $T_{\text{sys}} = 500$  K, 250 K cases the measurement error is dominant at all altitudes (not shown).

The temperature retrieval accuracy is degraded at tropospheric altitudes where water vapor is abundant as shown in the “wet” retrieval scenarios. Almost no temperature information is obtained from the ROI near the surface. The WV retrieval is best for a moist atmosphere (tropical), with an error ratio below 0.2 for altitudes up to 5 km. Generally, reasonable WV information in the (ROI) data is available below 5–8 km. Strong correlations are found between the WV and the temperature retrieval. The primary interest should focus on the WV retrieval, since tropospheric WV is highly variable and poorly known.

## Conclusions

We have combined two highly synergistic instruments, a ROI and a PMI. We assumed the combined ROI-PMI sensor to be mounted on the ISS and computed the expected occultation events of the ROI. A sample of 30 measurement events was chosen, in order to cover the Earth representatively. We performed “dry” temperature retrievals, where only the temperature profile was determined. Additionally, we investigated three “wet” scenarios, retrieving temperature and WV VMR profiles.

“Dry” temperature can be derived between 0 and 90 km, with better than 1 km resolution at lower altitudes, which degrades to 5 km in the mesosphere. Assuming reasonably modern instruments, the accuracy is better than 1 K up to altitudes of 35 km, and better or near 4 K in the mesosphere. Including WV in the retrieval (“wet” scenarios) degrades the accuracy of the temperature retrieval at lower to mid-tropospheric altitudes where the amount of WV is significant. Generally, the error is still below 1 K, but approaches the *a priori* error of 2 K close to the ground level (indicating that almost no information about the temperature is available in a combined temperature/WV retrieval at ground level).

The WV retrieval results show that WV information is entirely provided by the ROI. The retrieval range for a moist (tropical) atmosphere is 0–8 km, while a dry (mid-latitude winter) atmosphere allows retrieval below 5 km only. The observation of a separate WV line by the PMI (e.g., near 183 GHz) would furnish highly complementary WV information at altitudes  $> 8$  km.

Overall, the favorable performance demonstrated by this study for a combined ROI-PMI sensor indicates that an installation of such instruments on the ISS or other LEO platforms is very recommendable. The ISS is a particularly suited platform for a proof-of-concept mission, since it enables convenient instrument access also during the mission.

**Acknowledgments.** The authors wish to thank G. Hartmann (MPAE Lindau/Harz, Germany) for many fruitful discussions on the ROI-PMI concept and for providing partial funding by purchase order no. 320771/336-23.06.1998 from MPAE Lindau/Harz. The authors furthermore thank J. Ramsauer (IGAM, Univ. of Graz, Austria) for his help in producing the simulated ROI data.

## References

- Bühler, S., *Microwave Limb Sounding of the Stratosphere and Upper Troposphere*, Berichte aus der Physik, ISBN 3-8265-4745-4, Shaker Verlag, 1999.
- Croskey, C., et al., The Millimeter-Wave Atmospheric Sounder (MAS): A shuttle based remote sensing experiment, *IEEE Trans. Geosci. Remote Sens.*, **40**, 1090–1100, 1992.
- GRAS-SAG, The GRAS instrument on METOP, *ESA/EUMETSAT Rep. (ESA No. VR/3021/PI, EUM No. EPS/MIS/IN/9)*, 38 p., ESA/ESTEC, Noordwijk, Netherlands, 1998.
- Hartmann, G., et al., Millimeter Wave Atmospheric Sounder (MAS Follow-on). Proposal to DLR (DARA), MPAE Lindau/Harz, D-37191 Katlenburg-Lindau, Germany, 9 pp.+annexes, 1997.
- Kirchengast, G., End-to-end GNSS Occultation Performance Simulator (EGOPS) overview and exemplary applications, *Wissenschaftl. Ber. No. 2/1998, 138 pp*, Inst. for Meteorol. and Geophys., Univ. of Graz, Halbaerthg. 1, A-8010 Graz, Austria, 1998.
- Kursinski, E., G. Hajj, J. Schofield, R. Linfield, and K. Hardy, Observing Earth’s atmosphere with radio occultation measurements using GPS, *J. Geophys. Res.*, **102**, 23,429–23,465, 1997.
- Palmer, P., J. Barnett, J. Eyre, and S. Healy, A non-linear optimal estimation inverse method for radio occultation measurements of temperature, humidity, and surface pressure, *J. Geophys. Res.*, **105**, 17,513–17,526, 2000.
- Rocken, C., et al., Analysis and validation of GPS/MET data in the neutral atmosphere, *J. Geophys. Res.*, **102**, 29,849–29,866, 1997.
- Rodgers, C. D., Characterization and error analysis of profiles retrieved from remote sounding measurements, *J. Geophys. Res.*, **95**, 5587–5595, 1990.
- von Engel, A., S. Bühler, J. Langen, T. Wehr, and K. Kunzi, Retrieval of upper stratospheric and mesospheric temperature profiles from Millimeter-Wave Atmospheric Sounder data, *J. Geophys. Res.*, **103**, 31,735–31,748, 1998.
- Ware, R., et al., GPS sounding of the atmosphere from Low Earth Orbit: Preliminary results, *Bull. Am. Meteorol. Soc.*, **77**, 19–40, 1996.

S. Bühler, A. von Engel, and K. Kunzi, Univ. of Bremen, Institute of Environmental Physics, Kufsteiner Strasse, D-28359 Bremen, Germany. (e-mail: sbuehler@uni-bremen.de; engeln@uni-bremen.de; kunzi@physik.uni-bremen.de)

G. Kirchengast, Institute for Geophysics, Astrophysics, and Meteorology, Univ. of Graz, Universitätsplatz 5, A-8010 Graz, Austria. (e-mail: gottfried.kirchengast@kfunigraz.ac.at)

(Received April 25, 2000; revised November 20, 2000; accepted November 24, 2000.)